Synthesis of Al-doped Zinc Oxide Nanoparticle (AZnO) Film Depositions and Characterization Using Sol–Gel Processing For Solar Cell Application

[1]MADHAVI PRASANGI, [2]Dr.N.JAYA MADHURI

[1]Research Scholar, Department of Physics, Jawaharlal Nehru Technological University, Ananthapuram, Andhra Pradesh, India
[2]Assistant Professor, NBKR Institute of Science And Technology, Vidyanagar, Nellore District, Andhra Pradesh, India

ABSTRACT: Over the past decade, there has been considerable focus on the synthesis of metal nanoparticles with distinct and exceptional characteristics, making it a highly captivating area of research. Among these nanoparticles, Zinc Oxide NanoParticles (ZnO NPs) have gather significant attention in the field of bioengineering. Various approaches have been explored for the preparation of ZnO nanoparticles, but the sol-gel method stands out as an economical and efficient chemical technique that offers the versatility to tailor the structural and optical properties of the NPs. Therefore, Synthesis of Al-doped Zinc Oxide Nanoparticle (AZnO) Film Depositions and Characterization Using Sol–Gel Processing For SolarCell Application is presented in this research. Here, zinc acetate salt and sodium hydroxide were used as precursors in the sol-gel process to first create ZnO NPs, which was then followed by the calcination of the precipitated material at 180ºC. Then sol–gel method is used in spin coating of AZnO thin films deposition on glass substrate using zinc acetate di-hydrate as a precursor with different molar concentrations. X-Ray Diffraction (XRD), UltraViolet-Visible spectroscopy (UV-vis), Transmission Electron Microscopy (TEM) and Scanning Electron Microscope (SEM) are used to investigate the structural, optical and morphological properties of synthesized ZnO NPs and AZnO films. With regard to using AZnO as a transparent conductive oxide for modern applications including displays, solar cells, and etc, the results of this investigation attracted a lot of interest.

KEYWORDS: Zinc Oxide NanoParticles (ZnO NPs), sol–gel method, Al-doped ZnO (AZnO) thin flms, Spin coating.

DOI: 10.48047/ecb/2023.12.5.503

I. INTRODUCTION

Today, the creation of nanoparticles with particular features is the more interesting and attractive aspect of study.

The oxide in nanoparticles attracts a lot of attention research fields because of its special features [1]. It is widely used as solar energy conversion, catalysis, varistors, gas sensors, non linear optics etc. ZnO nanostructures obtained a great attention in the research area because ZnO has large band gap. Zinc oxide is a highly applicable semiconductor material. Wide application of this nanomaterial is connected to wide spectrum of energy band gap, high bond energy, and great thermal conductivity but also with its non-toxicity, antibacterial activity, biocompatibility and biodegradability characteristics [2].

The creation of metal nanoparticles with particular and different features has received a lot of interest in recent years [3]. This has led to the development of a huge variety of techniques for synthesizing nanocompounds like solgel, solid state method, hydrothermal synthesis, electrospinning, electrodeposition, laser pyrolysis in the vapor phase, arc discharge, chemical vapor condensation, pyrolysis, thermal evaporation and much more [5,4]. The selection of synthesis method is closely related to the desired properties of material. ZnO nanoparticles may be made using a number of techniques, including the hydrothermal method, chemical vapour decomposition, the sol-gel approach, and thermal decomposition. The best approach among creating ZnO nanoparticles is the sol-gel method. The shape of the material may be studied and its size can be controlled during the fabrication of nanomaterials using the sol gel technique [6].

The group III elements that are most often employed to enhance the electrical and optical characteristics of ZnO are Gallium (Ga), Indium (In), or Aluminium (Al) [7]. Ga and precursors are often more costly than Al precursors. As a result, applying low doping percentages to achieve good physicochemical qualities may be possible with Al doping. The stability of resistivity is impacted by oxygen vacancy defects, which aluminium significantly reduces [8]. This analysis used the sol-gel technique to synthesize Al-doped ZnO film nanoparticles. Using a sintered target of sol-gel nanoparticles, radio frequency magnetron sputtering was used to create Al-doped Zinc Oxide (ZnO) coatings on glass substrates. X-ray diffraction and scanning electron microscopy were used to characterise the films.

II. LITERATURE SURVEY

A.R. Nimbalkar, N.B. Patil, V.V. Ganbavle, S.V. Mohite, K.V. Madhale, M.G. Patil et al [9], Aluminium-doped ZnO (AZO) thin films produced using the sol-gel spin coating method are displayed. Researchers looked at the way Al-doping affected the physicochemical and NO_2 (Nitrogen dioxide) sensing capabilities of AZO thin films. The zinc oxide phase development and the replacement of aluminium atoms into the zinc oxide lattice are confirmed by the structural and compositional investigation. At various operating temperatures, the gas detecting capabilities of AZO thin films were examined for NO_2 gas. The 2 at% AZO film sensor has good gas detecting properties at 200°C, according to the NO_2 sensing investigation.

S. Soren, S. Kumar, S. Mishra, P.K. Jena, S.K. Verma, P. Parhi et al [10], Utilizing the polyol method (organic phase) and room temperature precipitation (aqueous phase), monodispersed Zinc Oxide (ZnO) nanoparticles were produced, and their antibacterial and antioxidant capacity was assessed. Significant Metal Chelating (MC), DPPH (2,2-DiPhenyl-1-PicrylHydrazyl) free radical scavenging, hydroxyl radical, and superoxide radical scavenging activity (SAS) were all displayed by the synthesised ZnO nanoparticles. Scavenging activities were measured between 25 and 75ngml-1 concentration. When compared to particles made using the water precipitation approach, the Minimum inhibitory concentration (MIC) values of ZnO nanoparticles produced by the polyol approach were enhanced against both Gram-negative bacteria and Gram-positive. The results of the current study demonstrate that ZnO nanoparticles were effectively synthesised and that they were effective against a wide range of clinical bacterial infections due to their strong broad-spectrum antibacterial properties.

Priscy A. Luque, Osvaldo Nava, Gerardo Romo-Cardenas, Juan Ivan Nieto-Hipolito, Alfredo R. Vilchis-Nestor, Karla Valdez, Juan de Dios Sánchez-López, Fabian N. Murrieta-Rico et al. [11] published a analysis describing a simple synthesis procedure for producing zinc oxide nanoparticles utilising Citrus reticulata extract. For the zinc oxide nanoparticles, XRD only revealed the wurtzite structure, but TEM demonstrated size and shape homogeneity. Compared to commercial ZnO, the ZnO band gap was less. A waveguide model was examined using a computer simulation and electrical properties that depended on frequency. The results provide excellent parameters utilize in optoelectronic sensors. This method is non-toxic since there aren't many remaining green components in the ZnO NPs that are produced.

J.N Hasnidawani, Azlina, H. N., Norita, H., Bonnia, N. N., Ratim, S., & E. S. Ali et al.,[12] discuss into the Sol-gel method's use in the production of ZnO nanostructures. It is concluded that the sol gel approach was successful in producing ZnO nanoparticles. It creates nanorod-like structures with 84.98 nm-sized particles. S. Jurablu, M. Farahmandjou*and T. P. Firoozabadi et al. [13] discuss about that zinc oxide nanoparticles are made and investigate their structural and optical characteristics. The study's findings indicate that ZnO has a hexagonal wurtizite structure with a mean grain size of about 28 nm. It is evident from SEM photos that particles shapes change as temperature rises. The UV-Visible result reveals a 3.49ev (elecgron volts) larger band gap.

Riyadh M. Alwan, quraish A. Kadnim et al [14] Discussion about the analysis of ZnO nano-particles are using the sol-gel method. SEM, TEM, and XRD were used to characterize the ZnO nanoparticle. This study uses XRD to demonstrate particle size of 58.3 nm. Get a particle size range of 100–200 nm at 80 °C from SEM analysis. S.R.Brintha, M.Ajitha et al. [15] presented a research of ZnO nanoparticles made using the hydrothermal, sol-gel, and aqueous solution methods. XRD, SEM, EDX, and UV were used to characterize the synthesized particles. The synthesized ZnO nanoparticles possessed wurtzite structure, according to X-ray diffraction measurements, and their sizes ranged from 13 to 18 nm. The surface morphology of ZnO nanoparticles is spherical in the hydrothermal process and alters to flower-like arrangement in aqueous solution and sol-gel process, according to scanning electron microscopic analysis.

III. SYNTHESIS AND CHARACTERIZATION OF AZnO USING SOL-GEL PROCESS

3.1 Materials and methods

The precursors for ZnO were Zinc acetate dihydrate ($Zn(CH_3COOH)_2.2H_2O$), hydrochloric acid (HCl), Carboxy Methyl Cellulose (CMC), and sodium hydroxide (NaOH), while the precursors for ZnO and dopant precursors were zinc acetate dehydrate and aluminium nitrate nonahydrate, respectively, to prepare the sol-gel.

3.2 Synthesis of Zinc Oxide Nanoparticles (ZnO)

Using the sol-gel technique, ZnO nanoparticles were synthesised. In brief, to obtain a transparent solution, DeIonized (DI) water was used to dissolve 5.0g of zinc acetate dihydrate in 25ml over a duration of 30 minutes at 50°C. Next, 3.65ml of sodium hydroxide solution 12.5M (specified Molarity (M)) were slowly added to the solution, resulting in a white precipitate of zinc hydroxide.

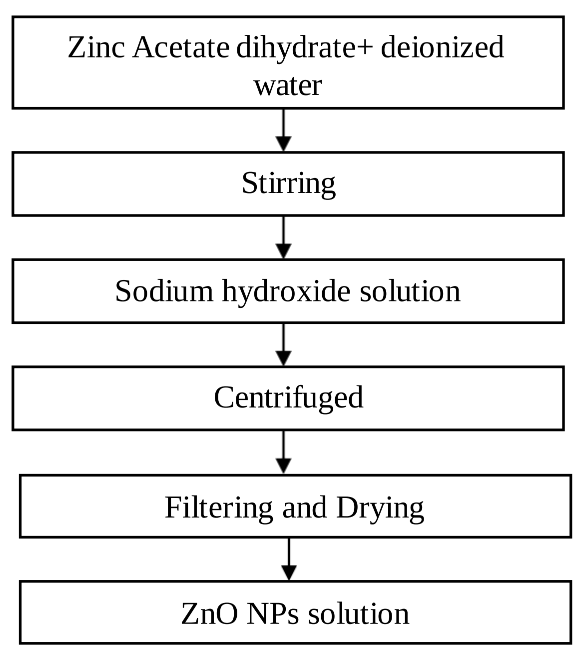

Fig. 1: SOL-GEL PROCESS OF ZINC OXIDE NANOPARTICLES SYNTHESIS

The precipitated solid was then collected by centrifuging the obtained suspension for 10 minutes at 8000 rpm (Revolutions per minute). After undergoing a second centrifugation to remove any remaining component, the recovered precipitate was three times resuspended in DI water. In order to create zinc oxide powder, the precipitate was calcined in a furnace (Nabertherm 1400, Germany) at a temperature of 180°C for one hour while being heated at a rate of 7°C/min. Glass pieces were coated with a solution containing various concentrations of synthesized ZnO NPs, and after 24 hours at 37°C, the suspension was added to an Escherichia coli (E. coli) culture to evaluate the ZnO NPs' antibacterial properties.

3.3 Synthesis of Al-doped Zinc Oxide Nanoparticles (AZnO)

The sol-gel technique was used to synthesize AZnO, with a range of 0.35 to 0.75 mol/L for the precursor concentration. First, 2-methoxyethanol (solvent) was used to dissolve zinc acetate dihydrate and aluminium nitrate nonahydrate. MonoEthanolAmine (MEA) was added in a few drops. A molar ratio of 1 was chosen between MEA and zinc acetate. In this analysis, MEA serves as a complexing agent. To create a clear, homogenous solution, the mixture was agitated for one hour at 60°C using a magnetic stirrer. 15 to 20 hours were given to the precursor solution to aging. In addition to employing DI water in an ultrasonic bath for 15 minutes, the substrates of Soda Lime Glass (SLG) were cleaned using methanol, ethanol, and again methanol for 10 minutes each. A spin coater (SPS SPIN 150) uses 3000 rpm for 30s at room temperature to deposit material. After each coating, synthetic films were warmed for five minutes in an oven (Binder, ED 53) set to 300 °C. It naturally cooled and dried. To enhance the thickness, this process was carried out five, ten, fifteen, and twenty times. As a result, samples with five different layer thicknesses the fifth, tenth, fifteenth, and twentieth were created for each concentration. For the purpose of crystallizing AZO, the films were then heated for one hour at 500°C in a closed N_2 atmosphere.

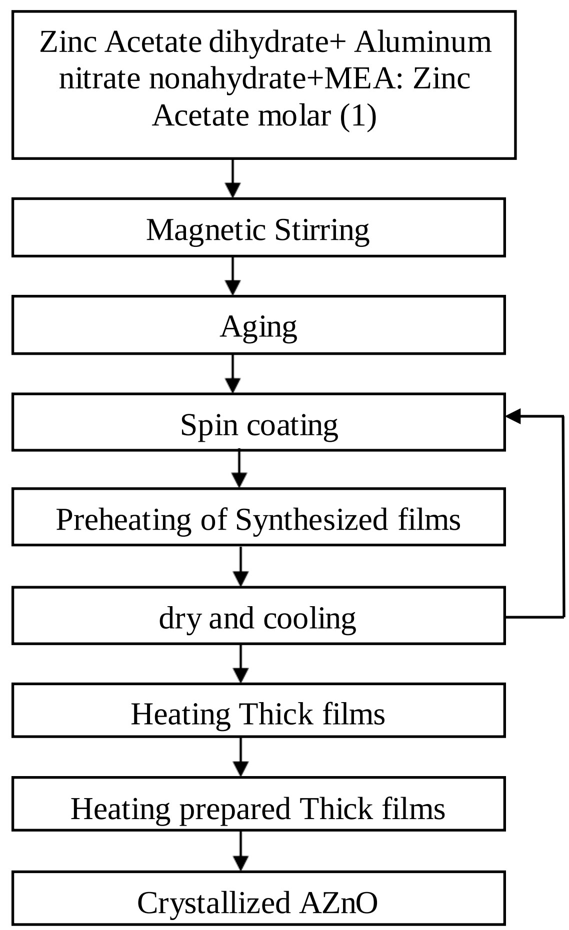

Fig. 2: SOL-GEL PROCESS OF Al-DOPED ZINC OXIDE NANOPARTICLES THIN FILMS

3.4 Characterization

In the phase of characterizing synthesized ZnO, to define the powder's phase composition and chemical composition was produced after calcination in the form of 15 KV Ni-filtered Cu-Kα. The synthesized powder's X-ray diffraction (XRD) pattern was recorded in the 28º to 70º diffraction angle range. Additionally, the peaks of the generated XRD pattern might be used to determine the information about crystalline size. Using Transmission Electron Microscopy (TEM), the morphology and size of zinc oxide were analyzed. In order to support the case for the creation of zinc oxide nanoparticles, an automated UV-vis spectrometer was used to measure the UV-vis absorption of zinc oxide dispersion across the wavelength range of 250 to 700 nm. UV spectra were examined using a ZnO suspension in DI water at a concentration of 100 g/ml.

During the characterization of synthesized AZnO surface profilometer was used to measure the film's thickness. Using an X-ray diffractometer, the structural characteristics of the Al-doped ZnO thin film created through sol-gel were examined. In order to investigate optical transmittance at the visible wavelength, it was done using a UV-visible spectrophotometer. Surface topography was examined using a Scanning Electron Microscope (SEM).

IV. RESULTS

4.1 Characterization of synthesized ZnO Structural properties: Figure 3's X-Ray Diffraction (XRD) pattern shows the existence of different diffraction peaks. These peaks match the zinc oxide structure seen in wurtzite, where zinc atoms are found in the tetrahedral positions of oxygen atoms that have been packed tightly into hexagonal shapes. No peak, as seen in Fig. 3, indicates the likelihood of contaminants present in the produced powder.

In other words, the outcome demonstrates the excellent purity of the synthesized ZnO. Additionally, Strong peaks in the pattern point to the previously mentioned highly crystallised and oriented nature of the synthesised zinc oxide.

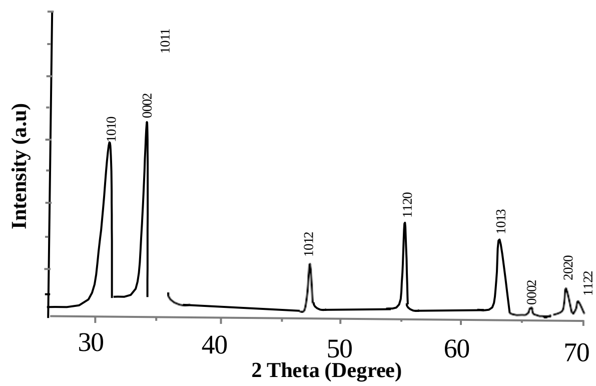

Fig. 3: X-Ray Diffraction of ZnO Powder Synthesized By Sol-Gel Method

Ultraviolet–Visible Spectroscopy: The ZnO suspension's UV-visible absorption spectrum (Fig. 4) shows an absorption peak at 360 nm that is part of a different band for ZnO. The XRD study of the purity of synthesized ZnO is substantially supported by this result. Although the ZnO nanoparticle's size of the UV-vis absorption band affects, it typically ranges from 330 to 380 nm. Here, the presence of a peak at 360 nm can serve as proof that ZnO NPs are present.

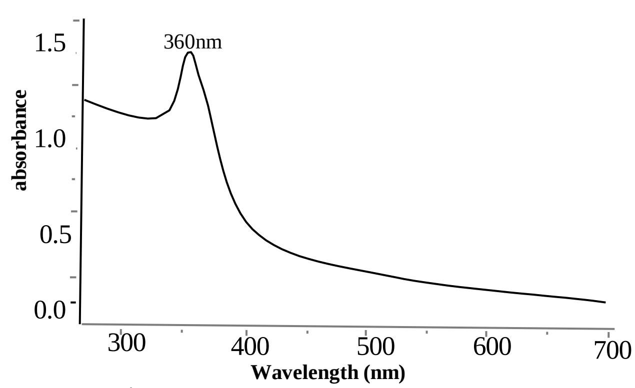

Fig. 4: UV-Vis absorption spectrum of synthesized ZnO NPs

Morphological properties: The TEM and SEM images of the ZnO-NPs made using the solgel technique are shown in Fig. 5 (A, and B). Due to their exceptional quality, the ZnO-NPs have evolved into an approximately hexagonal shape, as shown by the TEM in Fig. 5 A. The ZnO-NPs are seen in a 150,000X SEM micrograph in Figure 5B. The SEM image shows that ZnO-NPs are uniform in size and shape. Additionally, It shows that uniformly distributed ZnO-NP in powder form.

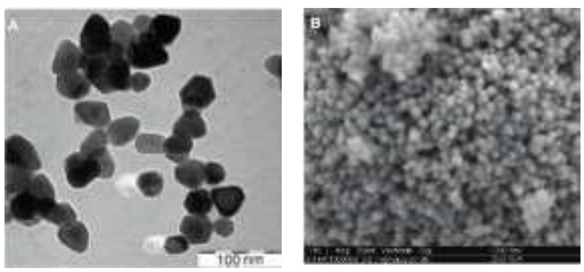

(A) Transmission electron micrograph, (B) scanning electron micrograph of the ZnO-NPs

Fig. 5: Morphology Image Of Zinc Oxide Nanoparticles (ZnO-NPs)

4.2 Characterization of synthesized AZO

Thickness: Fig. 6 demonstrates the sol-gel produced AZO thin film's thickness and the number of coated layers. It rises linearly from 295 to 1039 nm as the coating number increases.

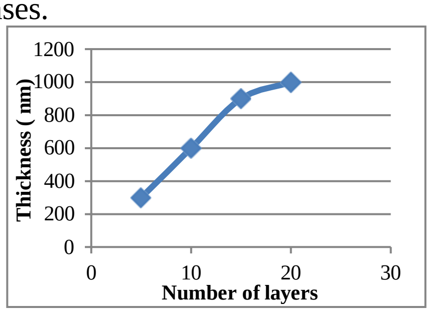

Fig. 6: Thickness Variance with The Number Of Layers

Structural properties: In Fig. 7, the XRD pattern for the AZO thin film was annealed at 500 °C is displayed. A dominant peak can be seen in the spectra around 34.60 degrees, which reflects the preferred orientation along the crystallographic axis (002). At axes (100) and (101), there are two further peaks at 31.80° and 36.30° with less intensity. C-plane orientation is preferred in every sample. This could be seen that as the film gets thicker, the peak intensity and sharpness get stronger. This peak sharpness indicates that as crystallite thickness increases, it also increases crystallite size.

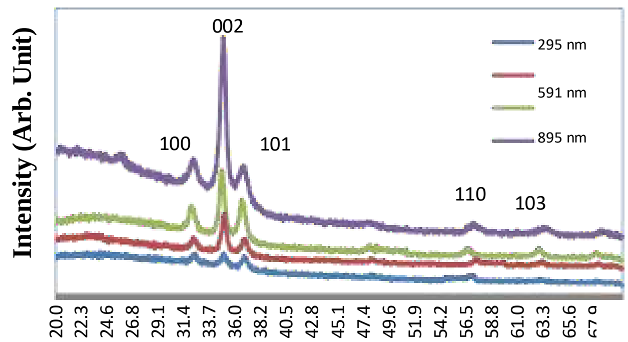

Fig. 7: X-ray Diffraction Spectra of AZO Film

Optical properties: The sharp increase in absorbance at $\lambda < 300$ nm is due to interband transitions at the fundamental edge. Band-gap energy increases with decreasing particle size due to quantum size effects. A decrease in absorbance at higher doping level of Al may be attributed to the decrease in the size of nanoparticles and increase in porosity which ultimately widens the band gap. The optical transmittances of Al doped Zno are 88% and 87% respectively. Optical transmittances of undoped ZnO is 93%. It shows clearly that the transmittance decreases with the increment of Al content. This suggests that Al ions are causing the formation of defect centres in host lattice (zinc oxide) proportionate to Al content. The decrease in band gap with increasing Aluminum concentration was due to the contributions of hybridization of electronic states, as well as the Aluminum-induced intensification of p-d repulsion and tensile strain.

SEM analysis: The surface topography of the films with the fifth, tenth, fifteenth, and twentieth layers is displayed in the SEM images in Fig. 10a–d. The substrate surface has been covered by the film, although much it seems rough. Wounds and voids can be seen in some areas. For water molecules and oxygen to enter the film, the voids are the preferred diffusion channel. As a result of the phenomenon, the AZO protecting is more resistant. In Fig. 10d, the unsymmetrical AZO rod is presented.

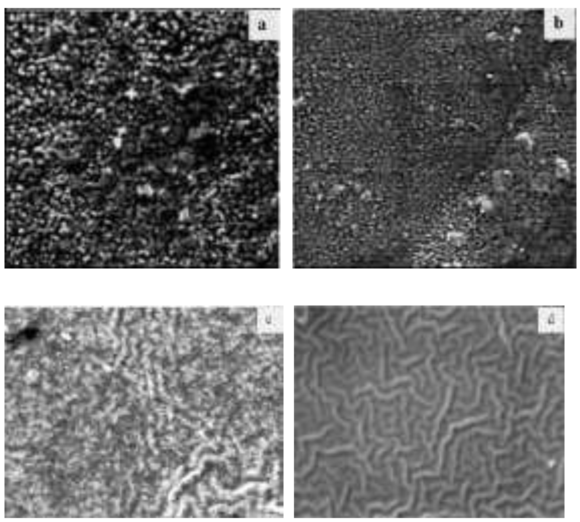

Fig. 10: SEM Images of AZO Film with Thickness of a-295 nm, b-591 nm, c-895 nm and d-1039 nm

V. CONCLUSION

This analysis came to the conclusion that the well-established synthesis technique for high-quality NPs, the sol-gel method of ZnO Nps. The synthesized ZnO NPs in the analysis were mostly close to hexagonal in shape, with particle sizes ranging from 300 to 700 nm. In addition, the ZnO NP suspension's UV-vis spectra showed an absorbance peak at 360 nm. A hexagonal wurtzite structure is evident from the structural features. Increasing the Zn content, the resistivity decreases as the carrier concentration increases. A decrease in absorbance at higher doping level of Al may be attributed to the decrease in the size of nanoparticles and increase in porosity which ultimately widens the band gap. SEM analysis reveals a non- uniform surface of the films. All of the films, nanoparticles, and sintered targets had hexagonal structures in the X-ray diffraction patterns that corresponded to the wurtzite phase. These films were compared to deposited using the sol-gel approach in terms of structural and optical performance.

VI. REFERENCES

[1] Eric Kwabena Droepenu , Boon Siong Wee, Suk Fun Chin, Kuan Ying Kok, Muhammad Firdaus Maligan, "Zinc Oxide Nanoparticles Synthesis Methods and its Effect on Morphology: A Review", Review, Volume 12, Issue 3, 2022, Biointerface Research in Applied Chemistry, 4261 – 4292

[2] B.S. Surendra, M.M. Swamy, T. Shamala, S. Rao, A.S. Sowmy, C. Mallikarjuna, S. Pramila, Development of enhanced electrochemical sensor and antimicrobial studies of ZnO NPs synthesized using green plant extract. Sensor Int. 3, 100176, 2022.

[3] P.S.K.N.K. Bhat, P. Nagaraju, "Fabrication of ultrasensitive hexagonal disc structured ZnO thin film sensor to trace nitric oxide", J. Asian Ceramic Society, 9 (1) (2021), pp. 96.

[4] Abhilash D. Jadhaoa, Sudhir Shendeb, Pramod Ingleb, Aniket Gadeb, Sunil W. Hajarec, Ranjit S. Ingole a, "Biogenic Synthesis of Zinc Oxide Nanoparticles by Bryophyllum pinnatum and its Acute Oral Toxicity Evaluation in Wistar Rats" 3, IEEE

Transactions on NanoBioscience, August 05,2020.

[5] M. I. Idris, Yasmin Zainol Abidin, Huda Abdullah, S. Shafie, Siti Amaniah Mohd Chachuli, M.Rashid, K. J. Xian, "Zinc Oxide Quantum Dots as Photoanode for DyeSensitized Solar Cell", 2020 IEEE International Conference on Semiconductor Electronics (ICSE), August 21,2020.

[6] R. Narzary, P. Phukan, S. Maity, and P. P. Sahu, "Enhancement of power conversion efficiency of Al/ZnO/p-Si/Al heterojunction solar cell by modifying morphology of ZnO nanostructure," J. Mater. Sci., Mater. Electron., vol. 31, no. 5, pp. 4142–4149, Mar. 2020

[7] Yuvaraj, S.; Fernandez, A.C.; Sundararajan, M.; Dash, C.S.; Sakthivel, P., "Hydrothermal synthesis of ZnO–CdS nanocomposites: Structural, optical and electrical behaviour. Ceramics Int. 2020, 46, 391-402.

[8] P. G. Ramos, E. Flores, C. Luyo, L. A. Sánchez, and J. Rodriguez, "Fabrication of ZnO-RGO nanorods by electrospinning assisted hydrothermal method with enhanced photocatalytic activity," Mater. Today Commun., vol. 19, pp. 407–412, Jun. 2019.

[9] A.R. Nimbalkar, N.B. Patil, \] V.V. Ganbavle, S.V. Mohite, K.V. Madhale, M.G. Patil, "Sol-gel derived aluminium doped zinc oxide thin films: A view of aluminium doping effect on physicochemical and NO2 sensing properties", Journal of Alloys and Compounds, Volume 775, 15 February 2019, Pages 466-473

[10] S. Soren, S. Kumar, S. Mishra, P.K. Jena, S.K. Verma, P. Parhi, "Evaluation of antibacterial and antioxidant potential of the zinc oxide nanoparticles synthesized by aqueous and polyol method", Microb. Pathogen., vol. 119, pp. 145-151, 2018

[11] Priscy A. Luque, Osvaldo Nava, Gerardo Romo-Cardenas, Juan Ivan Nieto-Hipolito, Alfredo R. Vilchis-Nestor, Karla Valdez, Juan de Dios Sánchez-López, Fabian N. Murrieta-Rico, "Facile zinc oxide nanoparticle green synthesis using Citrus reticulata extract for use in optoelectronic sensors", IEEE SENSORS JOURNAL, VOL. 21, NO. 10, 2017.

[12] J.N Hasnidawani, Azlina, H. N., Norita, H., Bonnia, N. N., Ratim, S., & E. S. Ali, "Synthesis of ZnO Nanostructures Using Sol-gel method" Procedia Chemistry, 19, 211–216,(2016).

[13] S. Jurablu, M. Farahmandjou*and T. P. Firoozabadi, "Sol-Gel Synthesis of Zinc Oxide (ZnO) Nanoparticles: Study of Structural and Optical Properties," Journal of Sciences, Islamic Republic of Iran 26(3) 281-285(2015)

[14] Riyadh M. Alwan, quraish A. Kadnim "Synthesis of Zinc Oxide Nanoparticle via sol-gel route and their characterization," 5(1), 1-6, (2015)

[15] S.R.Brintha, M.Ajitha, "Synthesis and characterization of ZnO nanoparticles via aqueous solution, sol-gel and hydrothermal methods", IOSR Journal of Applied Chemistry (IOSR-JAC) e-ISSN: 2278-5736.Volume 8, Issue 11 Ver. I (Nov. 2015), PP 66-72